Title

PTH treatment is effective in the Aga2/+ mouse model of moderate to severe osteogenesis imperfecta

Journal

Bone, 211

ISSN

8756-3282

Authors

Kot, Alexander
Wachtell, Davis
Wight, Caroline
et al.

Publication Date

2026-10-01

DOI

10.1016/j.bone.2026.117976

Bone 211 (2026) 117976

Contents lists available at ScienceDirect

Bone

journal homepage: www.elsevier.com/locate/bone

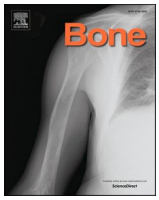

Full Length Article

PTH treatment is effective in the *Aga2/+* mouse model of moderate to severe osteogenesis imperfecta

Alexander Kot [a,b], Davis Wachtell [a], Caroline Wight [a], Roya Bagheri [a], Jennifer Zieba [a], Deborah Krakow [a,b,c,*]

[a] Orthopaedic Surgery, David Geffen School of Medicine at University of California at Los Angeles, Los Angeles, CA, USA
[b] Human Genetics, David Geffen School of Medicine at University of California at Los Angeles, Los Angeles, CA, USA
[c] Obstetrics and Gynecology, David Geffen School of Medicine at University of California at Los Angeles, Los Angeles, CA, USA

ARTICLE INFO

Keywords:
Osteogenesis imperfecta
Parathyroid hormone treatment
Mouse model
Microcomputed tomography
Three point bending
In vivo treatment
In vitro osteoblasts
Moderate severe OI

ABSTRACT

Osteogenesis imperfecta (OI) is a genetically heterogenous disorder characterized by brittle bone and recurrent fractures. The majority of OI is clinically categorized into mild, moderate, severe, and perinatal lethal forms. A clinical study on the use of intermittent parathyroid hormone (PTH) as an anabolic therapy for OI found PTH was effective in mild, but not in individuals with moderate/severe OI. However, this sub-group analysis was relatively small and considered preliminary by the authors. Since then, research on PTH therapy in OI has focused on mild OI and no studies of PTH use in moderate/severe OI patients or animal models have been reported. In this work, we used the *Aga2/+* mouse, an established autosomal dominant model of moderate/severe OI, to investigate whether PTH treatment has an effect on bone. *In vitro*, *Aga2/+* osteoblasts were sensitive to PTH and exhibited similar transcriptional changes compared to WT. *In vivo*, PTH treatment improved lumbar trabecular bone, increased cortical bone area fraction in the mid-femur, and, in females, led to improved biomechanical properties. These results demonstrate the *Aga2/+* model responded to PTH and support further investigation into whether PTH is effective in adult individuals with moderate/severe OI who have limited treatment options.

1. Introduction

Osteogenesis imperfecta (OI) is characterized by brittle bones with recurrent fractures due to impaired bone quantity and quality. OI is a genotypically heterogeneous skeletal disorder with causative variants in 22 different genes about 85% of which are caused by variants in genes encoding type I collagen alpha chains, *COL1A1* or *COL1A2* [1–4]. OI is also phenotypically heterogeneous and is clinically classified into mild (type I, OMIM#166200), moderate (type IV, OMIM#166220), severe (type III, OMIM#259420), perinatal lethal (type II, OMIM#166210) along with much rarer forms classified by disease genes (types V – XXIII). Loss of function or nonsense variants in *COL1A1* or *COL1A2* lead to quantitative defects in type I collagen and typically cause mild OI [5] whereas variants producing structural defects in type I collagen display much more phenotypic variability and often cause moderate, severe, or perinatal lethal OI [6]. While OI is a multisystem disorder, ongoing fractures in childhood and adulthood cause major morbidity and clinical care is focused on reducing fractures. To that end, there are no specific therapeutic agents approved for OI. Instead, drugs initially developed to treat osteoporosis are often used to increase bone mass and potentially reduce fractures.

Bisphosphonates are anti-resorptive agents that are commonly used in OI, particularly in children [7]. Bisphosphonates inactivate osteoclasts, inhibiting bone resorption to increase bone mineral density [8] and, although they increase bone mineral density in OI, it is unclear if they reduce the rate of fractures [7,9]. Further, as bisphosphonates reduce bone turnover and increase bone mineralization [8,10,11], it is possible they make OI bone even more brittle [9,12].

Alongside anti-resorptives, anabolic agents such as intermittent parathyroid hormone (PTH) and parathyroid related hormone (PTHrP) are used in osteoporosis to stimulate bone formation and increase bone density. PTH and PTHrP bind the parathyroid hormone 1 receptor (PTH1R), a G-protein coupled receptor, which then activates $G\alpha_s$ and adenylyl cyclase, increasing cyclic adenosine monophosphate (cAMP) levels and activating protein kinase A signaling [13,14]. PTH1R is expressed by cells from the osteoblast lineage and PTH regulates calcium

* Corresponding author at: Department of Orthopaedic Surgery, David Geffen School of Medicine at UCLA, 615 Charles E. Young Drive, BSRB/OHRC Room 510, Los Angeles, CA, 90095, USA.
E-mail address: dkrakow@mednet.ucla.edu (D. Krakow).

https://doi.org/10.1016/j.bone.2026.117976
Received 17 April 2026; Received in revised form 9 June 2026; Accepted 11 June 2026
Available online 12 June 2026

homeostasis by increasing bone resorption, indirectly stimulating osteoclasts through osteoblasts and osteocytes [13,15]. However, when given intermittently at low doses, PTH leads to an anabolic effect in the skeleton which underlies the rationale for its use in the treatment of osteoporosis [13,16].

In 2014, Orwoll et al. evaluated PTH treatment in adults with OI and found patients with mild OI had an anabolic response whereas patients with moderate/severe OI did not [17]. Importantly, the study was not powered for the moderate/severe subgroup analysis, genotypes were not reported, and the finding was considered preliminary. Possible explanations for these findings could be that structural defects in type I collagen may cause cellular dysfunction such as endoplasmic reticulum stress [18–20], which is worsened when osteoblasts are stimulated. Alternatively, transforming growth factor-beta receptor II (TGFβRII) is known to interact with PTH1R during endocytosis of the receptors to attenuate both pathways [21]. As increased levels of TGFβ have been reported in OI [22,23], this activity could produce a decrease in anabolic response to PTH [24,25]. Orwoll et al. specifically called for further clinical trials designed to identify if individuals with moderate and severe OI responds to PTH; however, to our knowledge, other studies investigating the anabolic effect of PTH alone in OI have only been conducted in mild OI [26,27]. Recently, another study by Hald et al. evaluated a combinatorial PTH and bisphosphonate treatment in adults with OI and found that patients receiving the treatment showed an anabolic response but with no change in fracture incidence. [28] However, most of the study cohort had mild OI (~75%) whereas those with moderate/severe OI were grouped as 'other' and not specifically analyzed. Thus, determining whether PTH induces an anabolic response in mouse models of moderate and severe OI will help to inform if further clinical studies should be pursued, particularly since few treatments are available for adults with OI, particularly the more severe forms.

In this study, we evaluated if PTH is an effective anabolic therapy in the *Col1a1*^{Aga2} (Aga2/+, *Col1a1* c.-16 T > A, exon 50) mouse model of moderate/severe OI (https://www.informatics.jax.org/allele/MGI:3769585) [18]. PTH treatment *in vitro* increased cAMP levels and induced gene transcription similarly in both *Aga2/+* and WT osteoblasts. Five weeks of PTH treatment *in vivo* improved *Aga2/+* lumbar trabecular bone parameters, increased cortical bone properties at the mid femur, and benefitted biomechanical properties of the femur. Together, this work demonstrates PTH is an effective therapy in this mouse model harboring a structural defect in type I collagen and supports further clinical investigation into the use of PTH in OI with qualitative type I collagen defects.

2. Methods

2.1. Animals

Aga2/+ mice (*Col1a1* c.-16 T>A, exon 50) were received as a gift from the C. Jacobsen laboratory and maintained on a C57BL/6J background [18]. For cell culture, mice were genotyped using TaqMan (Thermo Fisher Scientific) with the primer pair F: 5′-CCTCACTTCATTCCTACCTTGGTAA-3′ and R: 5′-CGGTGTGACTCTGGTGTGAAT-3′ and reporter sequences 5′-TCTCCCGCTGTCTTC-3′ and 5′-TCCCGCAGTCTTC-3′. Mice were housed in groups of 2–4 per cage within the University of California Los Angeles (UCLA) vivarium under a 12-h light/dark cycle, provided water and standard chow *ad libitum* (Lab Diet, 5053), and nesting material (Ancare, NES3600). These animal studies were performed under a protocol approved by the UCLA Research Safety and Animal Welfare Committee (ARC-2010-082).

2.2. Cell culture

Osteoblasts were isolated from 5-day old WT and Aga2/+ calvaria using collagenase IV digestion (Worthington Biochemical). For cAMP experiments, 5×10^4 cells/well were plated in 24-well plates, cultured for 48 h in DMEM (Cytiva, SH30243.01) + 10% FBS (Gibco, A31605–02, Lot U2938855RP) + penicillin/streptomycin, then cultured for 5 days in +10% FBS + 50 μg/mL ascorbic acid, 10 mM β-glycerophosphate, 10 nM dexamethasone + penicillin/streptomycin (osteogenic media). Wells were then washed with DMEM and incubated with hPTH (1–34) (escalating dose from 0 to 10,000 nM; Bachem, 4011474) in DMEM for 15 min before lysis and cAMP quantification by competitive enzyme immunoassay run in duplicate (R&D Systems, KGE012B). Total protein was assessed using the BCA reagent (Thermo Fisher Scientific). Prism 10 (GraphPad) was used to generate three parameter dose-response fits to calculate the half maximal effective concentration (EC50) for treated osteoblasts from each mouse.

For qPCR and western blot experiments, 100,000 cells were plated in 6-well plates, cultured for 48 h in DMEM + 10% FBS + penicillin/streptomycin, then cultured for 5 days in osteogenic media as described above. Wells were then washed with DMEM and incubated with 0 or 1 μM hPTH (1–34) in osteogenic media for 6 h before lysis in either Trizol (Invitrogen) or RIPA with inhibitors.

2.3. Western blot analyses

Calvaria protein lysates were boiled for 5 mins in Laemmli buffer (BioRad) with 2-mercaptoethanol, run on a 10% SDS-PAGE gel, transferred to a polyvinylidene difluoride membranes (Millipore Sigma), blocked using 5% milk in tris-buffered saline with 0.1% Tween 20, and probed overnight with a primary antibody: anti-ATF4 (Proteintech, 60035-1, 1:2000), anti-Caspase-12 (Cell Signaling Technology, 2202, 1:1000), anti-LC3 (Cell Signaling Technology, 12741, 1:1000), anti-BAD (Cell Signaling Technology, 9239, 1:1000), or anti-Vinculin (abcam, ab129002, 1:10000). Membranes were washed and probed using a peroxidase-conjugated secondary antibody: anti-rabbit IgG (Cell Signaling Technology, 7074, 1:2000) or anti-mouse IgG (Cell Signaling Technology, 7076, 1:2000), which was then detected using Pierce ECL or Supersignal West Femto Maximum Sensitivity Substrate (both Thermo Fisher Scientific). Images were captured using the ChemiDoc system (BioRad) and analysis was performed using ImageLab 6.1 (BioRad).

2.4. Quantitative PCR

Calvaria RNA was isolated using TRIzol (Invitrogen) following the manufacturer's instructions. DNA was digested using DNase I (Invitrogen) and complementary DNA (cDNA) was synthesized from 1 μg RNA using iScript Reverse Transcription Supermix (BioRad). Quantitative PCR was performed in triplicate using a QuantStudio 3 (Thermo Fisher Scientific) with Power Up SYBR Green (Applied Biosystems), 1 ng cDNA, and primer pairs listed in Supplemental Table 1. Hypothesis testing was performed using the ddCt method normalized to *B2m* expression, relative mRNA levels were calculated as 2^{-ddCt}.

2.5. In vivo PTH treatment

Three-month-old male and female WT and *Aga2/+* mice were randomized into PTH or vehicle treatment groups. The PTH group received subcutaneous hPTH (1–34) 60 μg/kg daily 5× per week (Bachem, 4011474) and the vehicle group received an equivalent volume of phosphate buffered saline. Mice were treated for 5 weeks and bodyweights were collected weekly. At sacrifice, mice were radiographed and dissected for tissue collection. Bones with callus or fractures were excluded from further characterization.

2.6. Micro-computed tomography (μCT)

Formalin fixed 5th lumbar vertebral body (LVB5) and femurs were imaged with a Skyscan 1272 μCT system (Bruker). Bones were held in saline soaked sponges, then scanned at 50 kV and 200 μA using an Al 0.5

mm filter, 2048 × 2048 detector, 950 ms exposure, 0.5° step, averaging over 3 frames with random motion, with a voxel size of 10 μm in each spatial direction. To calibrate bone mineral density, 300 and 1250 mg/cm^3 phantoms were imaged under the same settings. Two independent blinded observers analyzed the μCT images using CTAn (Brucker). Observers measured femur length using transaxial femur slices, femora with callus or fractures were excluded from the analysis. Trabecular bone was analyzed in the entire LVB5 vertebral body and in the distal femur starting 0.25 mm proximal to the growth plate, using a 2 mm long region of interest (ROI) containing the trabecular compartment. Cortical bone was analyzed at the mid-femur with a 0.5 mm long ROI. Femora with callus or fractures in the ROI were excluded from the analysis. Bone mineral density, tissue mineral density, trabecular microarchitecture, and cortical bone geometry were analyzed using standard methods [29]. Trabecular and cortical parameters derived from the femur were all normalized to total bone length. Thresholds corresponding to 719, 663 and 1205 mg/cm^3 were used for LVB5, distal femur, and mid-femur analysis, respectively.

2.7. 3-Point bending

This experiment was performed to determine biomechanical properties between treated and untreated bones. Dissected femurs were loaded to failure using an Instron 5943 using a 100 N load cell and displacement rate of 0.05 mm/s. All the samples were treated identically. Femurs were supported, but not fixed, on 2 points with a total span of 1 cm, an inner span of 0.7 cm, and a third point was lowered to load the bone, placing the anterior surface in compression and posterior surface in tension. Compressive force and displacement were measured at 50 Hz. Mechanical parameters including stiffness, yield, post-yield displacement, maximum load, work to failure were calculated from force *versus* displacement curves using custom-written MATLAB code [30]. Because the femora were not fixed, there could be variability in the data.

2.8. Statistical analysis

Prism 10 (GraphPad) was used for statistical analysis. After PTH stimulation, cAMP levels and EC50 were compared between WT and *Aga2/+* with *t*-tests. All other *in vitro* experiments were analyzed using

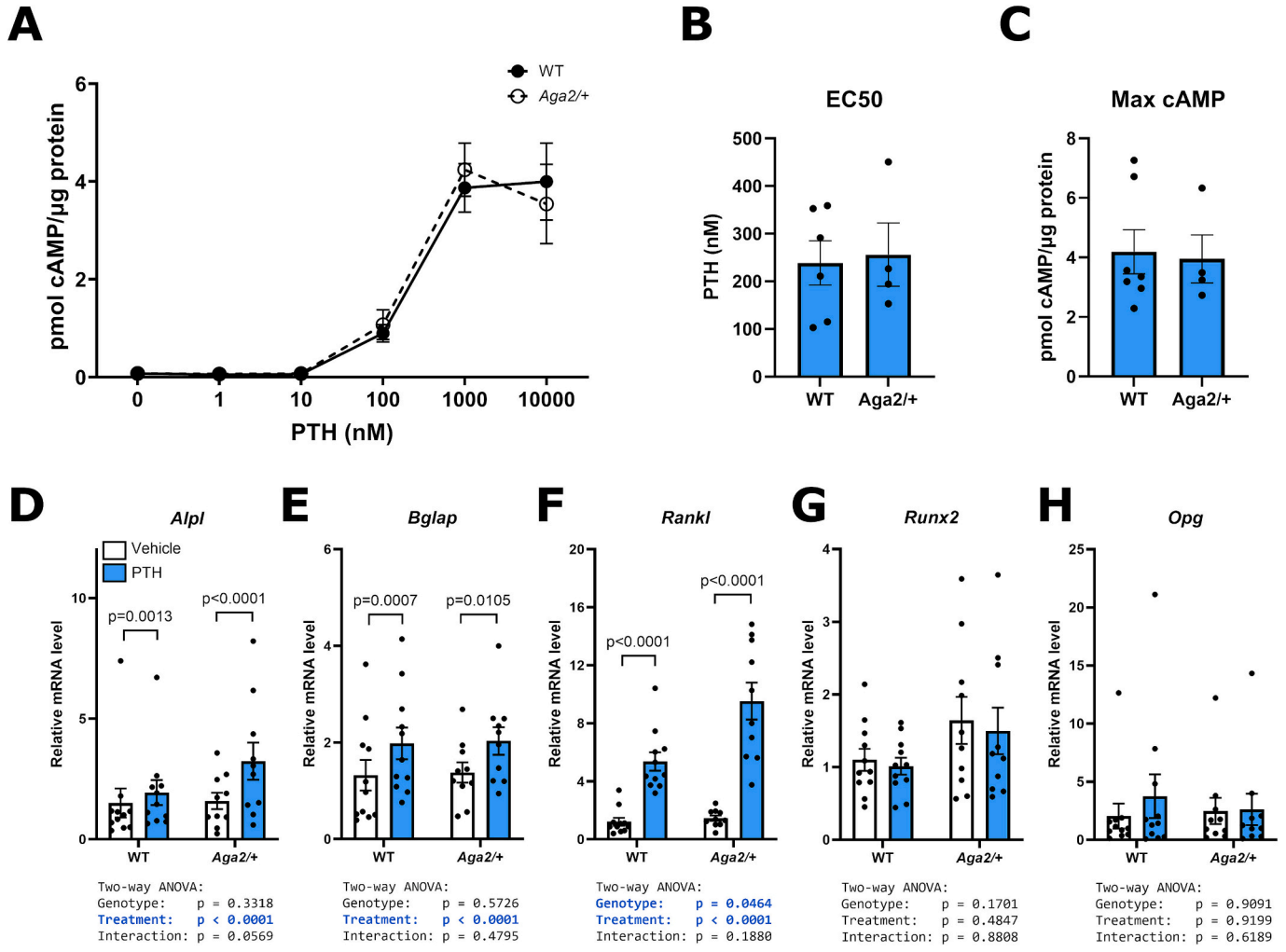

Fig. 1. Aga2/+ osteoblasts are sensitive to PTH *in vitro*. A: cAMP levels after 15 min of PTH treatment, normalized by total protein. B: Half effective maximal concentration (EC50). C: Maximum cAMP level measured, normalized by total protein. For the cAMP experiments, WT $n = 7$–10/PTH concentration and *Aga2/+* $n = 4$–6/PTH concentration. *t*-Tests were conducted with $p > 0.1$ for each comparison. D-H: qPCR analysis of osteoblasts after 6 h of 1 μM PTH or vehicle control. *Alpl*, *Bglap* (encodes osteocalcin), *Tnfsf11* (encodes RANKL), *Runx2*, and *Tnfrs11b* (encodes osteoprotegerin) normalized to *B2m* expression by ddCt. For qPCR experiments, WT $n = 11$/group, Aga2/+ $n = 10$/group, osteoblasts from each mouse were matched between vehicle and PTH treatments. Bar plots and error bars represent means ± SEM, dots represent independent replicates. 2-way ANOVA results below each plot, $p < 0.05$ highlighted. Post-hoc Šidák corrected comparisons shown above bars for $p < 0.1$.

repeated measures two-way ANOVA followed by Šidák corrected comparisons between vehicle and PTH treated groups of each genotype. Two-way ANOVA followed by Šidák corrected comparisons between vehicle and PTH treated groups of each genotype were used to analyze *in vivo* data. Fractures were analyzed using Mann-Whitney *U* tests. *p* values are shown for $0.001 < p < 0.05$ and $p < 0.05$ was considered statistically significant. Due to sexual dimorphism in the skeleton, males and females were analyzed and presented separately. Data are presented as group means ± SEM.

3. Results

3.1. In vitro, Aga2/+ osteoblasts are sensitive to PTH

PTH binds to PTH1R, a G-protein coupled receptor, activating $G\alpha_s$ and adenylyl cyclase, leading to increased levels of cAMP [14]. To assess the sensitivity of *Aga2/+* osteoblasts to PTH, primary osteoblasts were stimulated with increasing levels of PTH after which cAMP levels were quantified. Following 15 min of stimulation, there were no differences in cAMP levels between *Aga2/+* and WT osteoblasts, which were both increased in response to PTH stimulation (Fig. 1A). No differences between genotypes were detected in the EC50 or maximum cAMP levels (Fig. 1B, C). As 1 μM PTH resulted in a maximum cAMP response, it was selected as the dose for further *in vitro* stimulation experiments.

Downstream of the G-protein signaling cascades, PTH signaling modulates gene transcription. To assess whether *Aga2/+* osteoblasts exhibit the expected transcriptional response to PTH, mRNA levels of genes regulated by PTH signaling were analyzed using qPCR. Six hours of 1 μM PTH stimulation led to significantly increased *Alpl*, *Bglap* (encoding osteocalcin), and *Rankl* (*Tnsfs11*) expression (Fig. 1D–F). However, PTH treatment had no effect on *Runx2* or *Opg* (*Tnfrsf11b*) expression (Fig. 1G, H). Interestingly, two-way ANOVA identified Aga2/+ osteoblasts had significantly increased *Rankl* expression relative to WT (Fig. 1F). Overall, WT and *Aga2/+* osteoblasts exhibited a similar response of early PTH signaling and gene transcription.

Misfolded type I collagen accumulates in *Aga2/+* cells [18] and PTH could potentially worsen this accumulation. In WT osteoblasts, PTH treatment induces ER stress and activates the PKR-like endoplasmic reticulum kinase (PERK)-eukaryotic initiation factor 2α (EIF2A)-activating transcription factor 4 (ATF4) arm of the unfolded protein response [31]. Gene transcription and protein expression after 6 h of 1 μM PTH stimulation were analyzed for potential negative consequences.

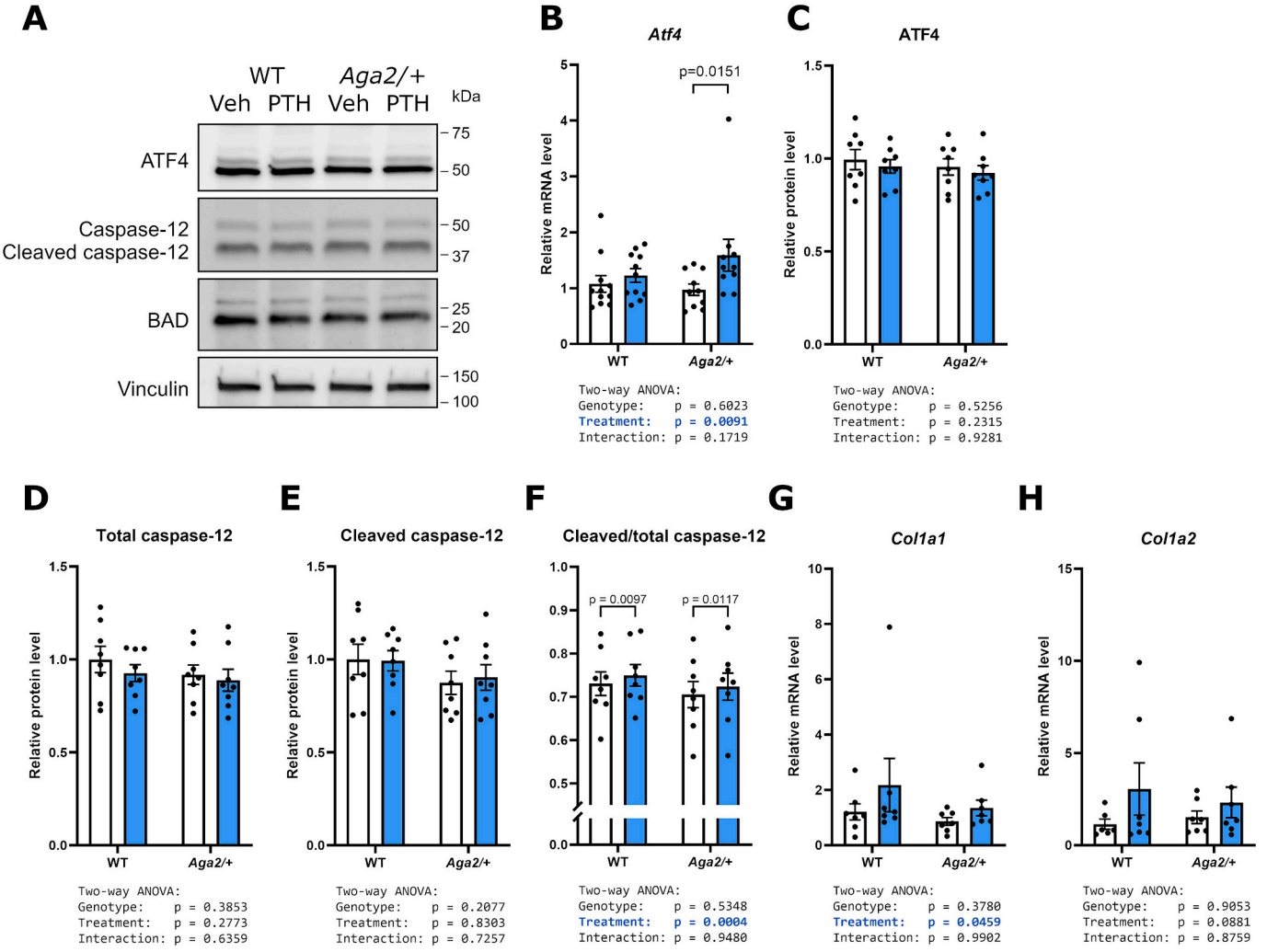

Fig. 2. PTH affects *Atf4* (unfolded protein response gene) in Aga2/+ osteoblasts with no change in autophagy or apoptosis markers. A: Representative blot image, protein collected from osteoblasts after 6 h of 1 μM PTH or vehicle control. B: qPCR analysis of *Atf4*, WT n = 11/group, Aga2/+ n = 10/group. C: WB analysis of ATF4. D-F: WB analysis of cleaved caspase-12, total caspase-12, and cleaved/total caspase-12. G-H: qPCR analysis of *Col1a1* (n = 7/group) and *Col1a2* (WT Vehicle *n* = 6, n = 7/group otherwise). For protein quantification, *n* = 8/group. Osteoblasts from each mouse were matched between vehicle and PTH treatments. Bar plots and error bars represent means ± SEM, dots represent independent replicates. 2-way ANOVA results below each plot, $p < 0.05$ highlighted. Post-hoc Šidák corrected comparisons shown above bars for $p < 0.1$.

Models of OI, including *Aga2/+*, have been reported to experience endoplasmic reticulum (ER) stress and activate the PERK arm of the unfolded protein response, leading to increased expression of ATF4 [20,32]. PTH increased *Atf4* gene expression when compared to vehicle control (Fig. 2B); however, there were no significant protein level differences in ATF4 (Fig. 2A, C). Chronically elevated ER stress can cleave and activate caspase-12, promoting apoptosis [33–36]. In both WT and *Aga2/+* osteoblasts, PTH treatment led to no differences in levels of total caspase-12 or cleaved caspase-12 (Fig. 2A, D–E). PTH treatment did lead to a significant increase in the ratio of cleaved to total caspase-12 in both WT and *Aga2/+* osteoblasts (Fig. 2F). As type I collagen is a major product of osteoblasts and the *Aga2/+* mice have a mutation in the *Col1a1* gene, we assessed the transcription of type I collagen genes. PTH treatment significantly increased *Col1a1* expression in both WT and *Aga2/+*, but not *Col1a2* expression (Fig. 2G–H). Overall, *Aga2/+* and WT osteoblasts had similar sensitivities to PTH, exhibiting similar transcriptional changes in response to short term PTH treatment. *Aga2/+* osteoblasts expressed significantly increased levels of *Atf4* mRNA; however, the treatment response of ATF4 and Caspase-12 were similar between WT and Aga2/+.

3.2. PTH treatment increases Aga2/+ trabecular bone

Since *Aga2/+* osteoblasts responded to PTH *in vitro*, an *in vivo* study was conducted. Male and female WT and *Aga2/+* mice were treated with PTH or vehicle control for 5 weeks. Using μCT analysis of the 5th lumbar vertebral body (LVB5), two-way ANOVA confirmed both male and female *Aga2/+* mice had reduced bone mineral density (BMD), bone volume fraction (BV/TV), trabecular thickness (TbTh), and trabecular number (TbN) as well as increased trabecular separation (TbSp), when compared to WT (Fig. 3).

Compared to Vehicle, PTH treated *Aga2/+* males had significantly increased LVB5 BMD and TbN, with trends of increased BV/TV and TbTh (Fig. 3A–E). Two-way ANOVA indicated PTH treatment significantly increased male BMD, BV/TV, and TbTh, without significant genotype-treatment interactions. *Aga2/+* females treated with PTH had significantly increased BMD, BV/TV, TbN, and significantly decreased TbSp, when compared to vehicle (Fig. 3A–C, E–F). Similarly, the significantly increased BMD, BV/TV, and TbN did not show significant genotype-treatment interactions indicating that both WT and *Aga2/+* are responding to the PTH treatment in a similar manner. A significant interaction was detected in TbSp where PTH treatment significantly decreased TbSp in *Aga2/+*, but not in WT females.

At the distal femur we found that compared to WT, both male and female *Aga2/+* mice had decreased BMD, BV/TV, TbN, and increased TbSp (Fig. 4A–D, F). There were no significant TbTh differences between WT and *Aga2/+* mice (Fig. 4A, E).PTH treatment significantly increased both WT and *Aga2/+* male TbTh and TbSp and significantly decreased WT TbN, without significant genotype-treatment interactions (Fig. 4A, D, F). No significant differences were detected between PTH and vehicle treated *Aga2/+* females (Fig. 4). Two-way ANOVA identified significant genotype-treatment interactions in BMD and TbN where PTH treatment led to significant increases in WT, but not in *Aga2/+* females (Fig. 4B, E).

3.3. PTH treatment improves Aga2/+ cortical bone and strength

Cortical bone was analyzed using μCT analysis of the mid-femur (Fig. 5A). *Aga2/+* mice had overall reduced cortical bone properties relative to WT. *Aga2/+* males had increased tissue mineral density (TMD), decreased polar moment of inertia (pMOI), and decreased cortical thickness (CtTh) compared to WT (Fig. 5B, D–E). Female *Aga2/+* mice had decreased cortical area fraction (CtAr/TtAr), pMOI, and CtTh compared to WT (Fig. 5C–E).

PTH treated *Aga2/+* males have increased CtAr/TtAr (Fig. 5A–C, Sup 2). PTH treatment significantly increased CtAr/TtAr as well as CtTh in both WT and *Aga2/+* males with no significant genotype-treatment interaction. PTH treated WT and *Aga2/+* females had significantly increased CtAr/TtAr, CtAr, and CtTh (Fig. 5A–E, Sup 2). WT females also showed increased pMOI following PTH treatment.

As PTH appeared to have a positive effect on *Aga2/+* cortical bone, we next analyzed the number of spontaneous fractures present at sacrifice. In males, PTH had no effect on the number of fractures observed at sacrifice (Fig. 6A). In females, vehicle treated mice had an average of 3 fractures (range 1–3) where PTH treated mice had an average of 2 (range: 1–6), with a trend toward statistical significance ($p = 0.0510$; Mann-Whitney *U* test).

To assess the impact of PTH on bone strength, 3-point bending was conducted on femurs collected from treated mice. Compared to WT, *Aga2/+* bone had significantly reduced stiffness, yield, post-yield displacement, ultimate force, and work to failure (Fig. 6B–F). In males, PTH had no significant treatment effect on any of the above mechanical parameters (Fig. 6B–F). PTH treated *Aga2/+* females, however, had significantly increased yield and ultimate force, with a trend of increased stiffness (Fig. 6B–D). Interestingly, a significant genotype-treatment interaction was observed, whereby PTH treatment led to reduced work to failure in WT females, but increased work to failure in *Aga2/+* females (Fig. 6F). Together, the fracture and mechanical testing results suggest that PTH treatment improved bone strength mainly in female mice.

4. Discussion

In a PTH treatment trial, an exploratory sub-group analysis of patients with moderate/severe OI suggested that intermittent PTH as an osteoanabolic therapy was ineffective. This study, however, was underpowered and definitive conclusions could not be made. We sought to determine if a mouse model of moderate/severe OI exhibited a positive response to PTH treatment, particularly because these patients have limited treatments options for their bone phenotype.

We identified that PTH led to increased expression of *Alpl*, *Bglap* (encoding osteocalcin), and *Tnfsf11* (encoding RANKL) when compared to vehicle control in both WT and *Aga2/+* osteoblasts. However, PTH treatment in both *Aga2/+* and WT osteoblasts did not lead to changes in *Runx2* or *Tnfrsf11b* (encoding osteoprotegerin) expression. *Runx2* is reported to be upregulated by PTH [31,37,38], but a study using mouse primary osteoblasts also identified that PTH had no significant effect on *Runx2* expression [39]. Similarly, PTH is reported to decrease Tnfrsf11b expression [40,41], but a study in mouse bone marrow stromal cells found *Tnfrsf11b* expression was most sensitive to PTH treatment early in osteoblast differentiation [42]. It could be that the osteoblasts in this study were more mature, especially as they were collected from postnatal mice and cultured. Nonetheless, this study identified that overall, *Aga2/+* and WT osteoblasts exhibited a similar signaling and transcriptional response to PTH treatment.

Since we found *Aga2/+* osteoblasts responded to PTH *in vitro*, we conducted an *in vivo* study to determine if *Aga2/+* mice would respond to PTH treatment. An analysis of studies involving PTH treated mice from 2001 to 2020 identified the optimal PTH response was in 12-week old (mature adult) male mice treated with 5–6 weeks of 30–60 μg/kg PTH 5×/wk. [43]. These conditions have an important impact on the ability for a study to identify a response to PTH and we used these conditions in our experimental design. As PTH was developed for postmenopausal osteoporosis, the effect of age on response to PTH in humans is largely unknown. Future clinical studies of PTH in OI could further categorize adults into those attaining peak bone mass and those who have acquired peak bone mass.

Due to well established sexual dimorphism in the skeleton, we analyzed sexes separately and identified differences in response to PTH treatment. While PTH increased the quantity of bone at LVB5 and the mid-femur in both males and females, the effect on trabecular microarchitecture and cortical bone geometry was different between the sexes. At LVB5, PTH treatment increased TbN in females, but not in

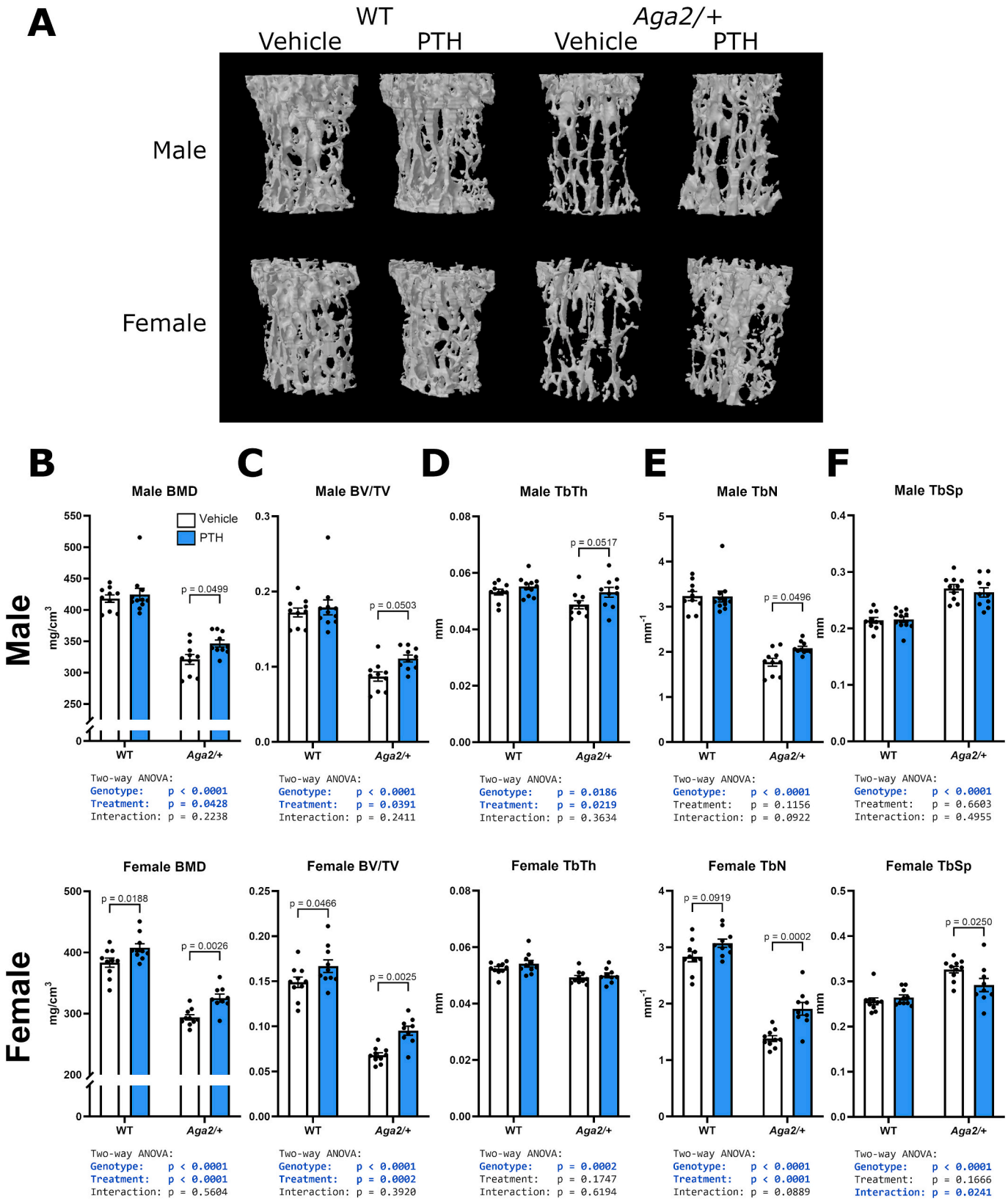

Fig. 3. PTH treatment increased LVB5 trabecular bone in Aga2/+ mice. A: Representative LVB5 reconstructions. B: Bone mineral density (BMD). C: Bone volume fraction (BV/TV). D: Trabecular thickness (TbTh). E: Trabecular number (TbN). F: Trabecular separation (TbSp). For males, WT $n = 10$/group, Aga2/+ vehicle $n = 11$, Aga2/+ PTH $n = 10$. For females, n = 10/group. Bar plots represent means ± SEM and dots represent independent replicates. 2-way ANOVA results below each plot, $p < 0.05$ highlighted. Post-hoc Šidák corrected comparisons shown above bars for $p < 0.1$.

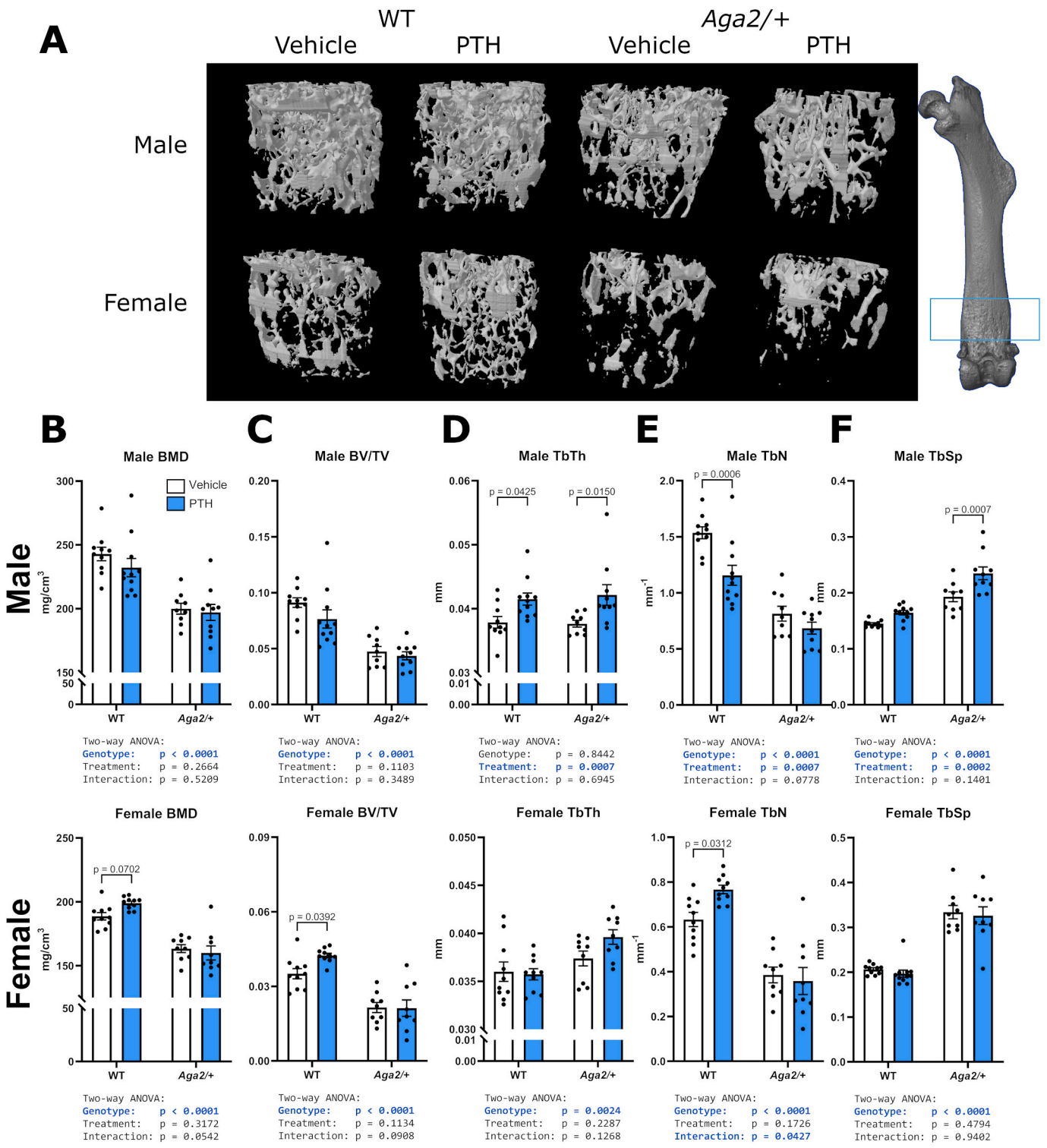

Fig. 4. PTH treatment impacted distal femur trabecular bone microarchitecture in Aga2/+ mice. A: Representative distal femur trabecular bone reconstructions. Right: Representative WT bone showing ROI used for trabecular measurements. B: bone mineral density (BMD). C: Bone volume fraction (BV/TV). D: Trabecular thickness (TbTh). E: Trabecular number (TbN). F: Trabecular separation (TbSp). For males, WT vehicle $n = 10$, WT PTH $n = 11$, *Aga2/+* vehicle $n = 9$, Aga2/+ PTH $n = 10$. For females, WT n = 10/group, Aga2/+ n = 9/group. Bar plots represent means ± SEM and dots represent independent replicates. Šidák corrected $p \leq 0.05$ are shown above bars.

males. Similarly, PTH treatment significantly decreased TbSp in *Aga2/+* females but not in males. In the distal femur, PTH increased male TbTh and TbSp, but reduced TbN whereas it significantly increased female TbN in WT mice only. Finally, 3-point bending identified that PTH significantly improved female, but not male femur biomechanical properties (stiffness, yield, ultimate force). It is important to note this study was not designed to rigorously test whether there is a sex difference in response to PTH and formal statistical testing for sex differences was not conducted. Nonetheless, these data suggest the way in which male and female bone respond to PTH treatment may differ.

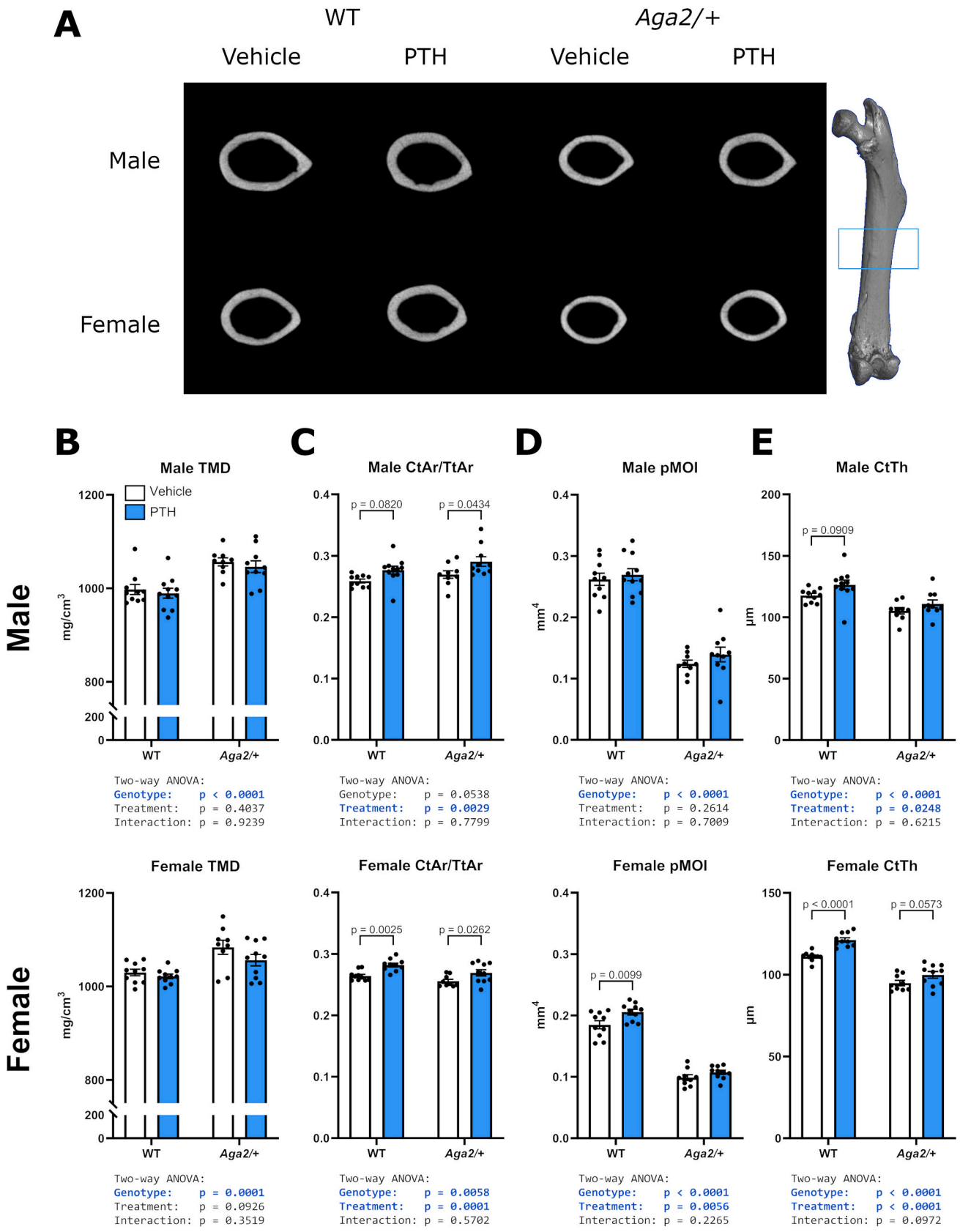

Fig. 5. PTH treatment improved mid-femur cortical bone in Aga2/+ mice. A: Representative mid-femur cross-section. Right: Representative WT bone showing ROI used for cortical measurements. B: tissue mineral density (TMD). C: Cortical area per tissue area (CtAr/TtAr). D: Polar moment of inertia (pMOI). E: Cortical thickness (CtTh). For males, WT vehicle n = 10, WT PTH n = 11, Aga2/+ vehicle n = 9, Aga2/+ PTH n = 10. For females, WT n = 10/group, Aga2/+ vehicle n = 9, Aga2/+ PTH n = 10. Bar plots represent means ± SEM and dots represent independent replicates. 2-way ANOVA results below each plot, $p < 0.05$ highlighted. Post-hoc Šidák corrected comparisons shown above bars for $p < 0.1$.

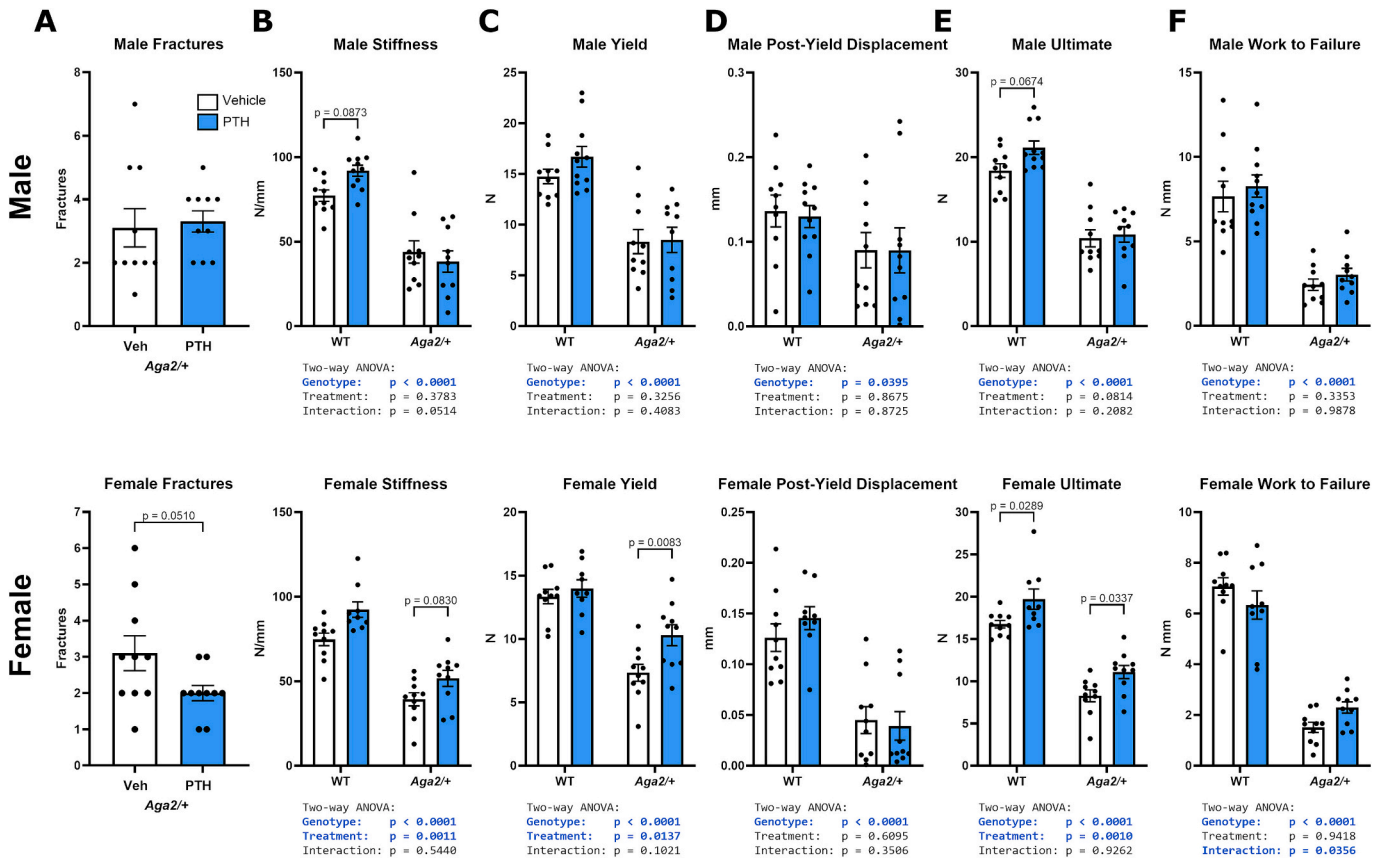

Fig. 6. PTH improved bone strength in female *Aga2/+* mice. A: Long bone fractures at day 35 of treatment. No fractures were detected in WT mice (n = 10–11/group). For Aga2/+, n = 10/group. Mann-Whitney *U* tests *p* values for $p < 0.05$ are shown. B: Stiffness *ex vivo* femurs analyzed by 3-point bending. C: Yield point. D: Post-yield displacement. E: Ultimate force. F: Work to failure. For 3-point bending, male WT vehicle n = 10, WT PTH n = 11, Aga2/+ vehicle and PTH n = 10. Female WT vehicle n = 10, WT PTH n = 9, Aga2/+ vehicle and PTH n = 10. Bar plots represent means ± SEM and dots represent independent replicates. 2-way ANOVA results below each plot, $p < 0.05$ highlighted. Post-hoc Šidák corrected comparisons shown above bars for $p < 0.1$.

The effect of PTH was also dependent on the skeletal site analyzed. Site specific responses have been previously reported and loading conditions may play a role in PTH's anabolic effect [44]. PTH treatment led to increased LVB5 trabecular bone in both WT and *Aga2/+* mice but only increased distal femur trabecular bone in the WT females. This site specificity has important implications for how responsiveness to PTH is clinically monitored. Dual-energy X-ray absorptiometry (DXA) is used clinically to quantify areal BMD at low-cost and low radiation doses [45]. DXA assessment can be affected by fractures, bone deformities, implanted hardware, as well as bone diameter and does not differentiate cortical from trabecular bone [45]. As individuals with OI can experience frequent fractures requiring surgical intervention, bony deformities, and short stature, it may not be possible to perform DXA at the same site for all OI patients in a clinical trial. Alternatives such as quantitative computed tomography may be a better technique to characterize the skeletal response to PTH.

There are some limitations to our study. The experimental design utilized treatment of naive mice whereas many patients with moderate/severe OI may have a history of bisphosphonate use. Bisphosphonates are powerful bone remodeling inhibitors [8] and, based on experiments focused on osteoporosis, it is possible that PTH treatment may be less effective in an individual with suppressed bone turnover [46–48]. While this study found that PTH increased both trabecular and cortical bone properties, there was only a trend toward a significant decrease in spontaneous fractures. These fractures occurred at unknown timepoints under uncontrolled loading conditions and had been healing for an undetermined amount of time, thus they might be an unreliable measure of bone strength. Instead, we conducted biomechanical testing and found that in *Aga2/+* females, PTH resulted in a stronger bone as treatment increased stiffness, yield point, and ultimate force.

This work shows that osteoblasts from the *Aga2/+* mouse model of moderate to severe OI responded to PTH *in vitro* and PTH improved bone properties in *Aga2/+* mice *in vivo*. We highlighted important sex difference in the murine response to PTH and characterized the differences in response to PTH across multiple skeletal sites. As there are few treatment options for individuals with OI and PTH is a preferred therapy for osteoporosis with very high fracture risk [49,50], these findings strongly support further investigation of PTH treatment in mouse models of OI. Additionally this study supports revisiting the preliminary clinical sub-group results reported by Orwoll et al. in 2014 and the clinical trial results reported recently by Hald et al. in 2026 [17,28], with a study powered and designed specifically to identify whether individuals with moderate or severe OI respond to PTH therapy.

CRediT authorship contribution statement

Alexander Kot: Writing – review & editing, Writing – original draft, Visualization, Methodology, Investigation, Funding acquisition, Formal analysis, Data curation, Conceptualization. **Davis Wachtell:** Investigation. **Caroline Wight:** Investigation. **Roya Bagheri:** Writing – review & editing, Visualization, Methodology, Investigation. **Jennifer Zieba:** Writing – review & editing, Investigation, Conceptualization. **Deborah Krakow:** Writing – review & editing, Investigation, Funding acquisition, Conceptualization.

Funding

This work was supported by NIH F30HD113414, T32GM008042, and T32GM152342 awarded to AK.

Declaration of competing interest

Nothing to disclose.

Acknowledgements

This work was supported by NIH F30HD113414, T32GM008042, and T32GM152342. The content is solely the responsibility of the authors and does not necessarily represent the official views of the National Institutes of Health. Deborah Krakow is supported by the Joshua S. and Beth C. Friedman Chair in Women's Genetic Research.

Appendix A. Supplementary data

Supplementary data to this article can be found online at https://doi.org/10.1016/j.bone.2026.117976.

Data availability

Data will be made available on request.

References

[1] F. Rauch, F.H. Glorieux, Osteogenesis imperfecta, Lancet Lond. Engl. 363 (2004) 1377–1385, https://doi.org/10.1016/S0140-6736(04)16051-0.
[2] A. Forlino, W.A. Cabral, A.M. Barnes, J.C. Marini, New perspectives on osteogenesis imperfecta, Nat. Rev. Endocrinol. 7 (2011) 540–557, https://doi.org/10.1038/nrendo.2011.81.
[3] R. Morello, Osteogenesis imperfecta and therapeutics, Matrix Biol. 71–72 (2018) 294–312, https://doi.org/10.1016/j.matbio.2018.03.010.
[4] J. Dubail, P. Brunelle, G. Baujat, C. Huber, M. Doyard, C. Michot, P. Chavassieux, A. Khairouni, V. Topouchian, S. Monnot, E. Koumakis, V. Cormier-Daire, Homozygous loss-of-function mutations in CCDC134 are responsible for a severe form of osteogenesis imperfecta, J. Bone Miner. Res. 35 (2020) 1470–1480, https://doi.org/10.1002/jbmr.4011.
[5] M.C. Willing, S.P. Deschenes, R.L. Slayton, E.J. Roberts, Premature chain termination is a unifying mechanism for COL1A1 null alleles in osteogenesis imperfecta type I cell strains, Am. J. Hum. Genet. 59 (1996) 799–809.
[6] N. Garibaldi, R. Besio, R. Dalgleish, S. Villani, A.M. Barnes, J.C. Marini, A. Forlino, Dissecting the phenotypic variability of osteogenesis imperfecta, Dis. Model. Mech. 15 (2022) dmm049398, https://doi.org/10.1242/dmm.049398.
[7] K. Dwan, C.A. Phillipi, R.D. Steiner, D. Basel, Bisphosphonate therapy for osteogenesis imperfecta, Cochrane Database Syst. Rev. 10 (2016) CD005088, https://doi.org/10.1002/14651858.CD005088.pub4.
[8] S. Ma, E.L. Goh, A. Jin, R. Bhattacharya, O.R. Boughton, B. Patel, A. Karunaratne, N.T. Vo, R. Atwood, J.P. Cobb, U. Hansen, R.L. Abel, Long-term effects of bisphosphonate therapy: perforations, microcracks and mechanical properties, Sci. Rep. 7 (2017) 43399, https://doi.org/10.1038/srep43399.
[9] S.H. Ralston, M.S. Gaston, Management of osteogenesis imperfecta, Front. Endocrinol. 10 (2020), https://doi.org/10.3389/fendo.2019.00924 (accessed October 14, 2022).
[10] P. Roschger, S. Rinnerthaler, J. Yates, G.A. Rodan, P. Fratzl, K. Klaushofer, Alendronate increases degree and uniformity of mineralization in cancellous bone and decreases the porosity in cortical bone of osteoporotic women, Bone 29 (2001) 185–191, https://doi.org/10.1016/s8756-3282(01)00485-9.
[11] G.Y. Boivin, P.M. Chavassieux, A.C. Santora, J. Yates, P.J. Meunier, Alendronate increases bone strength by increasing the mean degree of mineralization of bone tissue in osteoporotic women, Bone 27 (2000) 687–694, https://doi.org/10.1016/s8756-3282(00)00376-8.
[12] D.B. Burr, Fifty years of bisphosphonates: what are their mechanical effects on bone? Bone 138 (2020) 115518 https://doi.org/10.1016/j.bone.2020.115518.
[13] B.C. Silva, A.G. Costa, N.E. Cusano, S. Kousteni, J.P. Bilezikian, Catabolic and anabolic actions of parathyroid hormone on the skeleton, J. Endocrinol. Investig. 34 (2011) 801–810, https://doi.org/10.3275/7925.
[14] R.W. Cheloha, S.H. Gellman, J.-P. Vilardaga, T.J. Gardella, PTH receptor-1 signalling—mechanistic insights and therapeutic prospects, Nat. Rev. Endocrinol. 11 (2015) 712–724, https://doi.org/10.1038/nrendo.2015.139.
[15] T.J. Martin, PTH1R actions on bone using the cAMP/protein kinase a pathway, Front. Endocrinol. 12 (2022), https://doi.org/10.3389/fendo.2021.833221.
[16] H. Dobnig, R.T. Turner, The effects of programmed administration of human parathyroid hormone fragment (1-34) on bone histomorphometry and serum chemistry in rats, Endocrinology 138 (1997) 4607–4612, https://doi.org/10.1210/endo.138.11.5505.
[17] E.S. Orwoll, J. Shapiro, S. Veith, Y. Wang, J. Lapidus, C. Vanek, J.L. Reeder, T. M. Keaveny, D.C. Lee, M.A. Mullins, S.C.S. Nagamani, B. Lee, Evaluation of teriparatide treatment in adults with osteogenesis imperfecta, J. Clin. Invest. 124 (2014) 491–498, https://doi.org/10.1172/JCI71101.
[18] T.S. Lisse, F. Thiele, H. Fuchs, W. Hans, G.K.H. Przemeck, K. Abe, B. Rathkolb, L. Quintanilla-Martinez, G. Hoelzlwimmer, M. Helfrich, E. Wolf, S.H. Ralston, M. Hrabé de Angelis, ER stress-mediated apoptosis in a new mouse model of osteogenesis imperfecta, PLoS Genet. 4 (2008) e7, https://doi.org/10.1371/journal.pgen.0040007.
[19] L.S. Mirigian, E. Makareeva, E.L. Mertz, S. Omari, A.M. Roberts-Pilgrim, A. K. Oestreich, C.L. Phillips, S. Leikin, Osteoblast malfunction caused by cell stress response to procollagen misfolding in α2(I)-G610C mouse model of osteogenesis imperfecta, J. Bone Miner. Res. Off. J. Am. Soc. Bone Miner. Res. 31 (2016) 1608–1616, https://doi.org/10.1002/jbmr.2824.
[20] R. Besio, G. Iula, N. Garibaldi, L. Cipolla, S. Sabbioneda, M. Biggiogera, J.C. Marini, A. Rossi, A. Forlino, 4-PBA ameliorates cellular homeostasis in fibroblasts from osteogenesis imperfecta patients by enhancing autophagy and stimulating protein secretion, Biochim. Biophys. Acta (BBA) - Mol. Basis Dis. 1864 (2018) 1642–1652, https://doi.org/10.1016/j.bbadis.2018.02.002.
[21] T. Qiu, X. Wu, F. Zhang, T.L. Clemens, M. Wan, X. Cao, TGF-β type II receptor phosphorylates PTH receptor to integrate bone remodelling signalling, Nat. Cell Biol. 12 (2010) 224–234, https://doi.org/10.1038/ncb2022.
[22] I. Grafe, T. Yang, S. Alexander, E. Homan, C. Lietman, M.M. Jiang, T. Bertin, E. Munivez, Y. Chen, B. Dawson, Y. Ishikawa, M.A. Weis, T.K. Sampath, C. Ambrose, D. Eyre, H.P. Bächinger, B. Lee, Excessive TGFβ signaling is a common mechanism in osteogenesis imperfecta, Nat. Med. 20 (2014) 670–675, https://doi.org/10.1038/nm.3544.
[23] I.-W. Song, S.C. Nagamani, D. Nguyen, I. Grafe, V.R. Sutton, F.H. Gannon, E. Munivez, M.-M. Jiang, A. Tran, M. Wallace, P. Esposito, S. Musaad, E. Strudthoff, S. McGuire, M. Thornton, V. Shenava, S. Rosenfeld, S. Huang, R. Shypailo, E. Orwoll, B. Lee, Targeting TGF-β for treatment of osteogenesis imperfecta, J. Clin. Invest. 132 (2022) e152571, https://doi.org/10.1172/JCI152571.
[24] W. Liu, B. Lee, S.C.S. Nagamani, L. Nicol, F. Rauch, E.T. Rush, V.R. Sutton, E. Orwoll, Approach to the patient: pharmacological therapies for fracture risk reduction in adults with osteogenesis imperfecta, J. Clin. Endocrinol. Metab. 108 (2023) 1787–1796, https://doi.org/10.1210/clinem/dgad035.
[25] I. Grafe, J. Zieba, E. Munivez, Y. Chen, M.-M. Jiang, B. Dawson, C. Jiang, A. Castellon, J. Sliepka, S.C.S. Nagamani, B. Lee, TGF-beta inhibition restores the responsiveness to osteoanabolic PTH treatment in the Crtap−/− model of recessive osteogenesis imperfecta, J. Bone Miner. Res. 33 (2018) 1076.
[26] D. Gatti, M. Rossini, O. Viapiana, M.R. Povino, S. Liuzza, E. Fracassi, L. Idolazzi, S. Adami, Teriparatide treatment in adult patients with osteogenesis imperfecta type I, Calcif. Tissue Int. 93 (2013) 448–452, https://doi.org/10.1007/s00223-013-9770-2.
[27] P.T. Leali, M. Balsano, G. Maestretti, M. Brusoni, V. Amorese, E. Ciurlia, M. Andreozzi, G. Caggiari, C. Doria, Efficacy of teriparatide vs neridronate in adults with osteogenesis imperfecta type I: a prospective randomized international clinical study, Clin. Cases Miner. Bone Metab. 14 (2017) 153–156, https://doi.org/10.11138/ccmbm/2017.14.1.153.
[28] J.D. Hald, C.J. Weir, C. Keerie, L. Dewar, M. MacLean, L. Milne, R. Keen, J. S. Walsh, K.E.S. Poole, B.L. Langdahl, J.R. Lindsay, N. Ghouri, R. Hollick, T. Aspray, R.K. Crowley, M. Cohen-Solal, Z. Hassan-Smith, S. Tuck, E.M. Curtis, N. C. Harvey, E.M.W. Eekhoff, J. Feenstra, G. Hampson, M. Stone, J. Turton, P. Patel, M. Siddiqi, R. Munro, M. Roy, Z. Paskins, D. Narayanan, E. Malcolm, M.K. Javaid, P. Osborne, J.C.Y. Tang, W. Lam, D. Moore, H.A. Black, A.D. Duckworth, N. S. Makaram, T. Guo, G. Stenhouse, S.H. Ralston, TOPaZ Investigators, Teriparatide plus zoledronic acid for osteogenesis imperfecta: a randomized clinical trial, JAMA (2026) e266889, https://doi.org/10.1001/jama.2026.6889.
[29] M.L. Bouxsein, S.K. Boyd, B.A. Christiansen, R.E. Guldberg, K.J. Jepsen, R. Müller, Guidelines for assessment of bone microstructure in rodents using micro–computed tomography, J. Bone Miner. Res. 25 (2010) 1468–1486, https://doi.org/10.1002/jbmr.141.
[30] K.J. Jepsen, M.J. Silva, D. Vashishth, X.E. Guo, M.C. van der Meulen, Establishing biomechanical mechanisms in mouse models: practical guidelines for systematically evaluating phenotypic changes in the diaphyses of long bones, J. Bone Miner. Res. Off. J. Am. Soc. Bone Miner. Res. 30 (2015) 951–966, https://doi.org/10.1002/jbmr.2539.
[31] K. Zhang, M. Wang, Y. Li, C. Li, S. Tang, X. Qu, N. Feng, Y. Wu, The PERK-EIF2α-ATF4 signaling branch regulates osteoblast differentiation and proliferation by PTH, Am. J. Physiol. Endocrinol. Metab. 316 (2019) E590–E604, https://doi.org/10.1152/ajpendo.00371.2018.
[32] I. Duran, J.H. Martin, M.A. Weis, P. Krejci, P. Konik, B. Li, Y. Alanay, C. Lietman, B. Lee, D. Eyre, D.H. Cohn, D. Krakow, A chaperone complex formed by HSP47, FKBP65, and BiP modulates telopeptide lysyl hydroxylation of type I procollagen, J. Bone Miner. Res. 32 (2017) 1309–1319, https://doi.org/10.1002/jbmr.3095.
[33] N. Morishima, K. Nakanishi, H. Takenouchi, T. Shibata, Y. Yasuhiko, An endoplasmic reticulum stress-specific caspase cascade in apoptosis: cytochrome c-independent activation of caspase-9 by caspase-12, J. Biol. Chem. 277 (2002) 34287–34294, https://doi.org/10.1074/jbc.M204973200.
[34] T. Yoneda, K. Imaizumi, K. Oono, D. Yui, F. Gomi, T. Katayama, M. Tohyama, Activation of caspase-12, an endoplastic reticulum (ER) resident caspase, through tumor necrosis factor receptor-associated factor 2-dependent mechanism in response to the ER stress, J. Biol. Chem. 276 (2001) 13935–13940, https://doi.org/10.1074/jbc.M010677200.

[35] E. Szegezdi, U. Fitzgerald, A. Samali, Caspase-12 and ER-stress-mediated apoptosis: the story so far, Ann. N. Y. Acad. Sci. 1010 (2003) 186–194, https://doi.org/10.1196/annals.1299.032.
[36] E. Fujita, Y. Kouroku, A. Jimbo, A. Isoai, K. Maruyama, T. Momoi, Caspase-12 processing and fragment translocation into nuclei of tunicamycin-treated cells, Cell Death Differ. 9 (2002) 1108–1114, https://doi.org/10.1038/sj.cdd.4401080.
[37] S. Yu, R.T. Franceschi, M. Luo, X. Zhang, D. Jiang, Y. Lai, Y. Jiang, J. Zhang, G. Xiao, Parathyroid hormone increases activating transcription factor 4 expression and activity in osteoblasts: requirement for osteocalcin gene expression, Endocrinology 149 (2008) 1960–1968, https://doi.org/10.1210/en.2007-1573.
[38] B. Arumugam, M. Vishal, S. Shreya, D. Malavika, V. Rajpriya, Z. He, N.C. Partridge, N. Selvamurugan, Parathyroid hormone-stimulation of Runx2 during osteoblast differentiation via the regulation of lnc-SUPT3H-1:16 (RUNX2-AS1:32) and miR-6797-5p, Biochimie 158 (2019) 43–52, https://doi.org/10.1016/j.biochi.2018.12.006.
[39] Regulation of osterix (Osx, Sp7) and the Osx promoter by parathyroid hormone in osteoblasts, J. Mol. Endocrinol. 43 (5) (2009). https://jme.bioscientifica.com/view/journals/jme/43/5/197.xml. (Accessed 18 April 2025) (n.d.).
[40] Q. Fu, R.L. Jilka, S.C. Manolagas, C.A. O'Brien, Parathyroid hormone stimulates receptor activator of NFkappa B ligand and inhibits osteoprotegerin expression via protein kinase A activation of cAMP-response element-binding protein, J. Biol. Chem. 277 (2002) 48868–48875, https://doi.org/10.1074/jbc.M208494200.
[41] B. Okudan, B. Seven, A.Ç. Karcı, M.F. Kılınçkaya, M. Çapraz, T. Turhan, N.C. M. Gülaldı, Parathyroid hormone on osteoprotegerin levels in patients with primary hyperparathyroidism, Eurasian J. Med. 54 (2022) 225–228, https://doi.org/10.5152/eurasianjmed.2021.21197.
[42] J.C. Huang, T. Sakata, L.L. Pfleger, M. Bencsik, B.P. Halloran, D.D. Bikle, R. A. Nissenson, PTH differentially regulates expression of RANKL and OPG, J. Bone Miner. Res. 19 (2004) 235–244, https://doi.org/10.1359/JBMR.0301226.
[43] L.E. Zweifler, A.J. Koh, S. Daignault-Newton, L.K. McCauley, Anabolic actions of PTH in murine models: two decades of insights, J. Bone Miner. Res. 36 (2021) 1979–1998, https://doi.org/10.1002/jbmr.4389.
[44] A.M. Rooney, T.J. McNeill, F.P. Ross, M.P.G. Bostrom, M.C.H. van der Meulen, PTH treatment increases cortical bone mass more in response to compression than tension in mice, J. Bone Miner. Res. Off. J. Am. Soc. Bone Miner. Res. 38 (2023) 59–69, https://doi.org/10.1002/jbmr.4728.
[45] S. Gazzotti, R. Sassi, M.P. Aparisi Gómez, A. Moroni, E. Brizola, M. Miceli, A. Bazzocchi, Imaging in osteogenesis imperfecta: where we are and where we are going, Eur. J. Med. Genet. 68 (2024) 104926, https://doi.org/10.1016/j.ejmg.2024.104926.
[46] J.A. Gasser, M. Kneissel, J.S. Thomsen, L. Mosekilde, PTH and interactions with bisphosphonates, J. Musculoskelet. Neuronal Interact. 1 (2000) 53–56.
[47] D.M. Black, S.L. Greenspan, K.E. Ensrud, L. Palermo, J.A. McGowan, T.F. Lang, P. Garnero, M.L. Bouxsein, J.P. Bilezikian, C.J. Rosen, PaTH Study Investigators, The effects of parathyroid hormone and alendronate alone or in combination in postmenopausal osteoporosis, N. Engl. J. Med. 349 (2003) 1207–1215, https://doi.org/10.1056/NEJMoa031975.
[48] C. Zhang, C. Song, Combination therapy of PTH and antiresorptive drugs on osteoporosis: a review of treatment alternatives, Front. Pharmacol. 11 (2021), https://doi.org/10.3389/fphar.2020.607017.
[49] F. Cosman, E.M. Lewiecki, R. Eastell, P.R. Ebeling, S. Jan De Beur, B. Langdahl, Y. Rhee, G.E.-H. Fuleihan, D.P. Kiel, J.T. Schousboe, J.L. Borges, A.M. Cheung, A. Diez-Perez, P. Hadji, S. Tanaka, F. Thomasius, W. Xia, S.R. Cummings, Goal-directed osteoporosis treatment: ASBMR/BHOF task force position statement 2024, J. Bone Miner. Res. 39 (2024) 1393–1405, https://doi.org/10.1093/jbmr/zjae119.
[50] P.M. Camacho, S.M. Petak, N. Binkley, D.L. Diab, L.S. Eldeiry, A. Farooki, S. T. Harris, D.L. Hurley, J. Kelly, E.M. Lewiecki, R. Pessah-Pollack, M. McClung, S. J. Wimalawansa, N.B. Watts, American Association of Clinical Endocrinologists/American College of Endocrinology clinical practice guidelines for the diagnosis and treatment of postmenopausal osteoporosis—2020 update, Endocr. Pract. 26 (2020) 1–46, https://doi.org/10.4158/GL-2020-0524SUPPL.